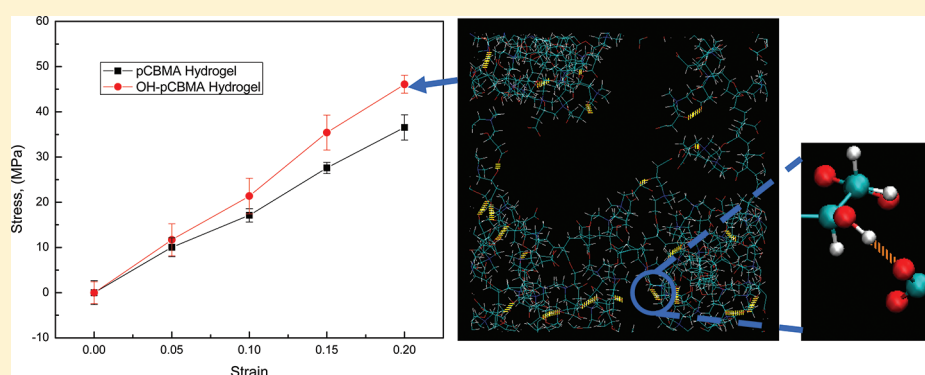


Improved Mechanical Properties of Zwitterionic Hydrogels with Hydroxyl Groups

Yi He,[†] Heng-Kwong Tsao,[‡] and Shaoyi Jiang*,[†][†]Department of Chemical Engineering, University of Washington, Seattle, Washington 98195, United States[‡]Department of Chemical and Materials Engineering, National Central University, Taoyuan 32001, Taiwan

ABSTRACT: Molecular dynamics simulations were performed to examine the mechanical properties of poly(carboxybetaine methacrylate) (pCBMA) hydrogels. pCBMA hydrogels with additional hydroxyl groups as physical cross-linkers (OH-pCBMA hydrogels) were studied for comparison. Results show that OH-pCBMA hydrogels have higher elastic modulus than pCBMA hydrogels. This improvement can be explained by hydrogen bond formation between hydroxyl groups and carboxylate groups in the OH-pCBMA hydrogel, which result in an enhanced polymer network within the hydrogel. The enhancement of the polymer work is also suggested by a smaller value of root-mean-square deviation of zwitterionic side chain pairs in the OH-pCBMA hydrogel than that in the pCBMA hydrogel. Additionally, the presence of hydrogen bonds leads to a lower equilibrium water content for the OH-pCBMA hydrogel compared to the pCBMA hydrogel, which is another reason for the greater mechanical modulus of the OH-pCBMA hydrogel.

INTRODUCTION

Hydrogels are water-swollen hydrophilic polymeric networks containing large amounts of water.^{1,2} As they can mimic the interstitial tissue environment, they have been widely used in many applications such as contact lenses and artificial corneas.^{3,4} Research in hydrogels, especially those made from zwitterionic materials such as poly(sulfobetaine methacrylate) (pSBMA) and poly(carboxybetaine methacrylate) (pCBMA), have attracted great attention in the past few years.^{5–7} Both pSBMA and pCBMA hydrogels were found to be highly fouling resistant.⁵ In recent work by Carr et al., pCBMA hydrogels with a new type of zwitterionic cross-linker have shown reduced cellular adhesion by about 90% relative to poly(2-hydroxyethyl methacrylate) (pHEMA) hydrogels.⁸ Moreover, unlike pHEMA, pCBMA hydrogels are readily functionalizable.^{8,9} Cellular adhesion on nonfouling pCBMA hydrogels can be promoted by adding cyclo(arginine-glycine-asparagine-D-tyrosine-lysine) peptide (cRGD).⁸

Aside from their fouling-resistant properties, stand-alone hydrogels with different mechanical properties can find uses in a wide range of applications, including cell cultures and nasal cartilage.¹⁰ The mechanical properties of hydrogels have significant effects on the cellular response of endothelial cells,

myocytes, hepatocytes, neural/glial cells, and chondrocytes.^{11–15} For instance, myoblasts can only form myotubes in striation on substrates with intermediate stiffness.¹² Glial cells, unlike neurons, were unable to survive in soft materials, an important distinction for designing materials to repair central nervous system injuries.^{11,13,16,17} Adjustment of mechanical properties can be achieved with various approaches.^{9,18,19} Further enhancement of the elastic modulus of hydrogels is often sought. Huang and co-workers incorporated hydrogel microspheres into bulk hydrogel structures and obtained a so-called macromolecular microsphere composite hydrogel.¹⁸ Because the external load on the hydrogel can be spread over many different chains, the hydrogel is less likely to form microcracks, preventing bulk failure and leading to improved mechanical strength. Another method to enhance the polymer network of hydrogels is to synthesize double-network hydrogels.^{20,21} Gong et al. demonstrated a method of obtaining tough hydrogels containing double-networks by controlling the ratio of the two networks.²⁰ The mechanical properties of the

Received: January 7, 2012

Revised: April 15, 2012

Published: April 17, 2012

hydrogel were improved by increasing the molar ratio of the highly cross-linked network to the loosely cross-linked network.

Recently, Carr and co-workers have shown that, by replacing the methacrylate backbone of pSBMA with a vinylimidazole backbone, they not only retained the nonfouling properties of the zwitterionic sulfobetaine group but also improved on the mechanical properties of the methacrylate backbone.¹⁹ The mechanical modulus of the poly(sulfobetaine vinylimidazole) (pSBVI) hydrogels, unlike the pSBMA hydrogels, is able to reach a range suitable for practical biological applications such as joint, ocular, and tissue engineering scaffolds. With the help of newly designed zwitterionic cross-linkers and a photopolymerization method, Carr and co-workers further improved the mechanical properties of pCBMA hydrogels (compressive modulus up to 90 MPa).⁹

Despite the significant progress made toward improving the mechanical performance of zwitterionic hydrogels, little is known about the molecular environment within hydrogels, especially the effects of introducing new chemical structures into the hydrogels. Molecular simulations are well suited to investigate the effects of chemical structures and guide experimental design to improve the performance of hydrogels.^{22–24} In this work, we will use two model hydrogels, pCBMA and hydroxyl group-containing pCBMA (OH-pCBMA) hydrogels as shown in Figure 1, to examine how

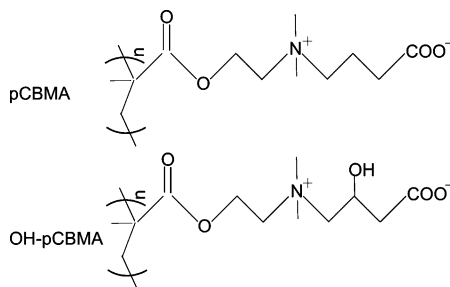


Figure 1. Structures of pCBMA and OH-pCBMA polymers.

the change in the molecular structure of zwitterionic repeating units will affect the mechanical properties of the pCBMA hydrogels. For each repeating unit in the OH-pCBMA hydrogels, a hydroxyl group was introduced to the carbon atom between positive and negative groups in each pCBMA repeat unit. The existence of these hydroxyl groups can lead to additional physical cross-linking between different zwitterionic side chains, which may further enhance the degree of cross-linking between zwitterionic charged pairs.²⁵ Therefore, it is likely that introducing hydroxyl groups to the pCBMA hydrogel may improve the mechanical properties. We will investigate how hydroxyl groups affect the equilibrium water content of zwitterionic hydrogels and their subsequent impacts on the mechanical properties of the hydrogels. Molecular insights will be provided through the analysis of interactions inside hydrogels.

SIMULATION DETAILS

OH-pCBMA hydrogels in this work were built with a similar approach reported in the study by Chiessi et al.²² This approach has previously been used to build pCBMA hydrogels.²⁶ The key for a hydrogel model is the creation of a three-dimensional networked structure. The polymer chains used in this simulation were built with Accelrys Material Studio

(version 3.2). The starting polymeric network includes three linear OH-pCBMA chains. Each of these chains has 15 repeating units in a fully extended conformation and a parallel orientation with respect to the Cartesian axes. Hydrophilic 1,3-dioxane cyclic junctions are used as cross-linkers in the hydrogel model. The same cross-linkers were also used in the study by Chiessi et al.²² For hydrogels used in biological applications, hydrophilic cross-linkers are desirable.⁹ There are two cross-linkers evenly embedded in each chain. These two cross-linkers are separated by five OH-pCBMA repeating units. Three other linear OH-pCBMA chains link the three main chains. Each chain is connected to the two different main chains so that a networked structure is formed. A perfect network structure is assumed in this study. Thus, no structural variations, such as free dangling chain ends and self-looping, exist in the simulation system. All three main chains in the system participate in forming the network structure through the periodic boundary conditions. The final configuration contains six chemical cross-linkers connecting six OH-pCBMA chains.

The polymer network was then solvated with various amounts of water molecules to obtain hydrogels with different water contents. All of the molecular mechanics (MM) and subsequent molecular dynamics (MD) simulations were performed with the large-scale atomic/molecular massively parallel simulator (LAMMPS) simulation package developed at Sandia National Laboratories.^{27,28} The equations of motion were integrated using the velocity-Verlet algorithm with a time step of 1.0 fs.²⁹ The Nose–Hoover temperature thermostat for the NVT and NPT MD simulations was used with a damping relaxation time of 0.1 ps. The particle–particle particle–mesh (PPPM) method was used to calculate the electrostatic interactions.³⁰ All of the systems were initially energy-minimized for 100 00 steps using the conjugate gradient algorithm to remove abnormally close contacts between molecules. After minimization, these systems were equilibrated through 500 ps of NVT MD simulations, followed by 4.5 ns of NPT MD simulations to obtain the fully relaxed hydrogel systems at 1 atm and 300 K. All data reported in this article were obtained from two individual MD simulations from two different initial configurations. All simulations were performed on a 5-node Intel quad-core Beowulf cluster running on Red Hat Enterprise Linux 4.

The all-atom consistent valence force field (CVFF),³¹ consisting of bond, Urey–Bradley, angle, dihedral, and improper terms, as well as nonbonded van der Waals (VDW) and Coulombic interactions, was used to describe the interactions in the polymer networks. The partial charges of each atom in the pCBMA polymer were obtained from previous work.²⁶ The partial charges of each atom in the OH-pCBMA polymer were calculated using the Jaguar program and shown in Figure 2 and Table 1.³² Calculations were carried out at the Hartree–Fock (HF) level using the 6-31G** basis set. In this procedure, the electrostatic field at a grid of points was calculated from the HF wave function. Using the grid points outside of the VDW radii, atom-centered charges are derived so as to match the HF potential while reproducing the dipole moment from HF. The water molecules are described with the extended simple point charge (SPC/E) model.³³

RESULTS AND DISCUSSION

Equilibrated Structures. In order to have a fair comparison between pCBMA and OH-pCBMA hydrogels, their mechanical properties need to be calculated when each

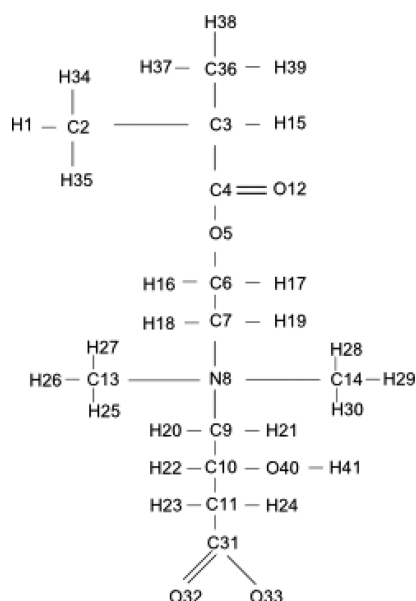


Figure 2. Definition of atom names in an OH-pCBMA monomer.

Table 1. Partial Charges of Atoms in an OH-pCBMA Monomer^a

atom	partial charge
C2	−0.509
H1, H34, H35	0.139
C36	−0.353
H37, H38, H39	0.099
C3	0.139
H15	0.035
C4	0.809
O12	−0.581
O5	−0.485
C6	0.171
H16, H17	0.064
C7	−0.080
H18, H19	0.115
C13, C14	−0.266
H25, H26, H27, H28, H29, H30	0.155
N8	0.070
C9	−0.251
H20, H21	0.151
C10	0.527
H22	−0.022
O40	−0.765
H41	0.448
C11	−0.449
H23, H24	0.095
C31	0.940
O32, O33	−0.803

^aThe atom names are defined in Figure 2.

hydrogel is under its respective equilibrium water content. As we discussed in previous work,²⁶ the equilibrium water contents can be found from the lifetime differences of zwitterionic physical cross-linkers in hydrogels under various water contents. This result was verified by free energy calculations with the new two-phase thermodynamics (2PT) method.³⁴ The calculated equilibrium water content is in good agreement with recent experiments.⁸ Using the same approach as before,²⁶ we

first calculated the autocorrelation function for the lifetime of zwitterionic side chain pairs to describe the stability of physical cross-linkers. The function was evaluated from the following expression:

$$C_{\text{pair}}(t) = \frac{1}{N_p} \sum_{i=1}^{N_p} \frac{\langle P(0)P(t) \rangle}{\langle P(0) \rangle^2}$$

where $P(t)$ is a binary function that equals 1 if the a zwitterionic side chain pair exists at time t , otherwise, $P(t)$ equals 0. N_p is the number of zwitterionic charged side chain pairs found in the hydrogel. The broken brackets ($\langle \rangle$) denote the ensemble average. A slower decay in the lifetime dynamics indicates a more stable association between zwitterionic side chain pairs. The distance to determine whether a zwitterionic side chain pair forms was determined from the first minimum of the radial distribution function of negatively charged groups around positively charged groups as shown in the previous work.²⁶

Figure 3a show the lifetime autocorrelation function for OH-pCBMA hydrogels at various water contents. The results clearly show that the lifetime of zwitterionic pairs decreases much

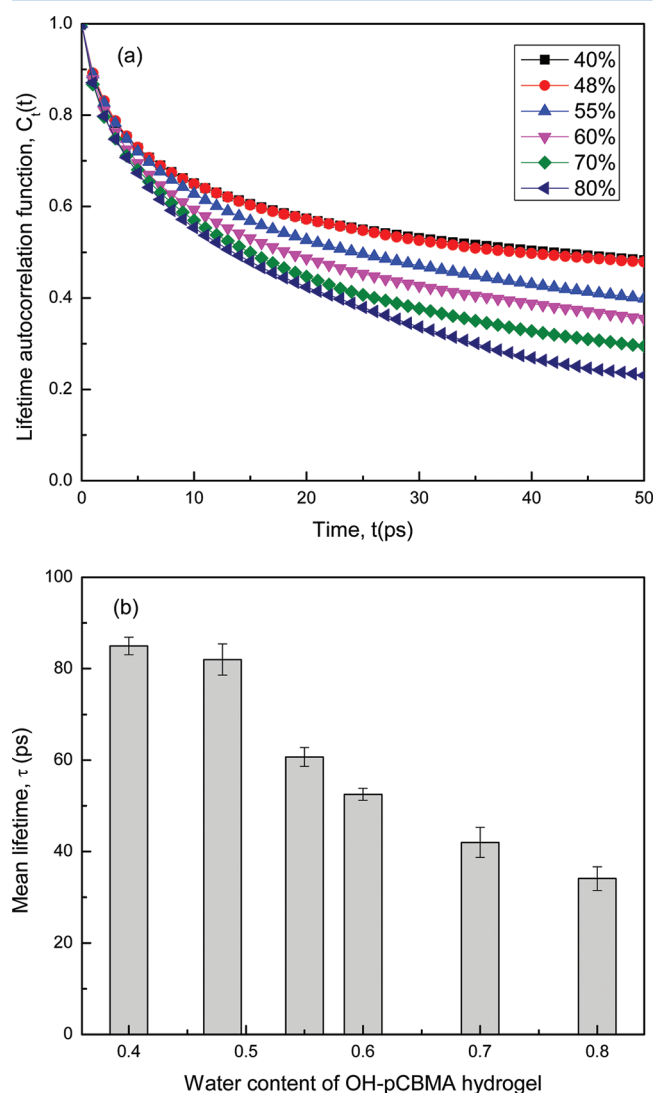


Figure 3. (a) Lifetime autocorrelation functions and (b) mean lifetimes of side chain pairs in the OH-pCBMA hydrogels at various water contents.

faster when its water content goes beyond 48% (by mass percentage) (Table 2). However, when water contents are

Table 2. Water Content of the OH-pCBMA Hydrogel with 60 Repeating Units^a

water content of hydrogel	number of water molecules
40%	592
48%	819
55%	1131
61%	1396
70%	2120
80%	3630

^aThe water content is defined by the mass percentage of water over the total mass of the hydrogel.

lower than 48%, the curves for the lifetime of zwitterionic pairs are almost identical. In order to quantitatively measure this difference, the mean lifetime was obtained by fitting an exponential decay function to the $C_{\text{pair}}(t)$ curve as follows:

$$C_{\text{pair}}(t) = A_p \exp\left(-\frac{t}{\tau_p}\right)$$

where A_p is the fitting constant, and τ_p is the mean lifetime of side chain pairs. The calculated mean lifetimes in Figure 3b confirmed a large drop at 48% water content. This means that the physical cross-linkers inside the hydrogels were disrupted by the presence of extra water molecules in the hydrogels. These results indicate that the equilibrium water content, where maximal swelling occurs, for zwitterionic OH-pCBMA hydrogels is 48%. When water content is larger than 48%, the lifetime drops and is expected to gradually decrease due to the increasing volume of hydrogel with additional water. For comparison, in our previous study,²⁶ the equilibrium water content of a pCBMA hydrogel was determined to be 62%. Thus, introducing hydroxyl groups as physical cross-linkers into pCBMA hydrogel decreases the equilibrium water content. Moreover, when the water content of both hydrogels are below their respective equilibrium values, the lifetime of zwitterionic side chain pairs in OH-pCBMA hydrogels (~ 80 ps) is about two times longer than that in pCBMA hydrogels (~ 40 ps).²⁶ This indicates that the former has a stronger polymer network inside the hydrogel and thus may exhibit a higher mechanical modulus.

Mechanical Properties. In order to determine whether OH-pCBMA hydrogel indeed has a higher mechanical modulus than pCBMA hydrogel, both of the hydrogels were deformed uniaxially (x -axis direction) up to 20% of strain over a period of 1 ns to assess the elastic modulus of the hydrogels. This deformation was done continuously and uniformly to the simulation box, and all atom coordinates were scaled to the new box simultaneously. The volume of the simulation box was kept constant, while extending deformation occurred in the x -direction by reducing the dimensions in the other two directions. The restart files, which contain the positions and velocities for each atom, were saved at 0%, 5%, 10%, 15%, and 20% of strain. Each restart file was then relaxed through 20 ns of NVT MD simulations. The last 10.0 ns of NVT MD production simulations were analyzed to obtain the stress under various strains. All of the simulations were done at a constant temperature of 300 K.

The results in Figure 4 show that the OH-pCBMA hydrogel exhibits a larger elastic modulus than pCBMA hydrogel when

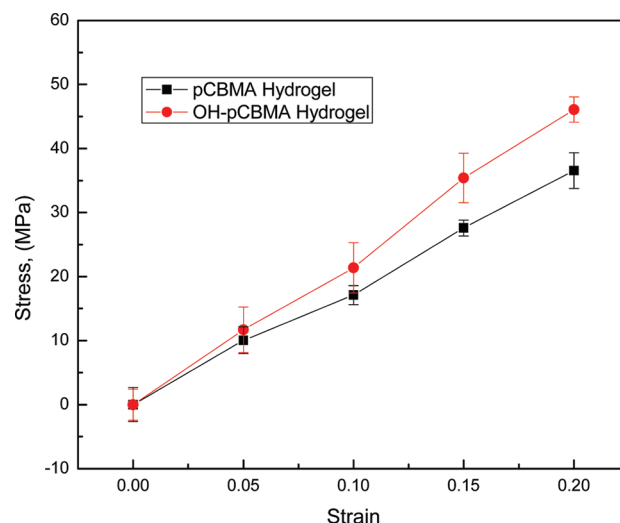


Figure 4. Comparison of stress vs strain curves for pCBMA hydrogel and OH-pCBMA hydrogel. The pCBMA hydrogel has a water content of 62%, while the OH-pCBMA hydrogel has a water content of 48%.

the same strain is applied. This enhanced mechanical modulus can be explained by hydrogen bonding between hydroxyl groups and carboxylate groups in the polymer network, as shown in Figure 5. In addition, the presence of hydrogen bonds leads to lower equilibrium water content for the OH-pCBMA hydrogel compared to the pCBMA hydrogel, which is another reason for the greater mechanical modulus of the OH-pCBMA hydrogel. The existence of these hydrogen bonds is consistent with the longer lifetime of zwitterionic side chain pairs in an

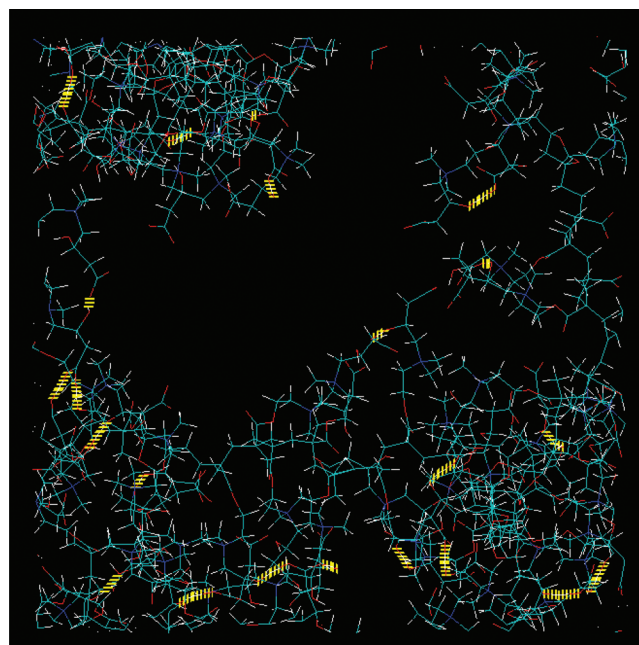


Figure 5. Simulation snapshot of the polymer network of an OH-pCBMA hydrogel (water is omitted for clarity). Hydrogen bonds between a hydrogen atom in a hydroxyl group and an oxygen atom in a carboxylate group are denoted with a yellow dotted line.

OH-pCBMA hydrogel than that in a pCBMA hydrogel, as shown in Figure 3b. In order to further confirm that the existence of the hydrogen bonds enhances the elastic modulus, the root-mean-square deviation (rmsd) of some heavy atoms (i.e., carbon atoms in carboxylate groups and nitrogen atoms in the quaternary amine groups) in the zwitterionic side chain pairs was calculated. Results in Table 3 show that the rmsd in

Table 3. Characteristics of Simulated Hydrogels^a

characteristics of hydrogels	pCBMA	OH-pCBMA
number of repeating units in hydrogel	60	60
number of cross-linkers in hydrogels	6	6
number of water molecules in hydrogels	1396	819
equilibrium water content of hydrogels	62%	48%
maximum strain applied to hydrogels	20%	20%
elastic moduli of hydrogels (MPa)	185.1 ± 3.1	239.0 ± 6.9
rmsd of side chain pairs	5.30 ± 0.13	4.11 ± 0.13

^aElastic moduli were calculated from the slope of the stress–strain curves in Figure 4. Values of the rmsd were calculated for carbon atoms in carboxylate groups and nitrogen atoms in the quaternary amine groups in zwitterionic side chain pairs.

OH-pCBMA was calculated to be 4.11 as compared to 5.30 in pCBMA. The lower value of the rmsd of OH-pCBMA represents a stronger polymer network, which is consistent with the presence of hydrogen bonding between hydroxyl groups and carboxylate groups in the hydrogel network.

CONCLUSIONS

In this work, molecular simulations were performed to study the mechanical moduli of zwitterionic pCBMA and OH-pCBMA hydrogels. It was found that the OH-pCBMA hydrogel containing additional hydroxyl groups has a greater elastic modulus than the pCBMA hydrogel. This enhancement in the mechanical modulus is due to the existence of hydrogen bonding between the hydroxyl groups and carboxylate groups in the OH-pCBMA hydrogel. These hydrogen bonds help form a stable and stronger polymer network in the OH-pCBMA hydrogel, leading to the improved mechanical modulus of the OH-pCBMA hydrogel.

AUTHOR INFORMATION

Corresponding Author

*Tel: 206-616-6509. Fax: 206-685-3451. E-mail: sjiang@u.washington.edu.

Notes

The authors declare no competing financial interest.

ACKNOWLEDGMENTS

We wish to thank Dr. Hong Xue for helpful discussion. We would like to thank the National Science Foundation (CMMI 0758358) and the American Chemical Society Petroleum Research Funds (ACS PRF #48096-AC7) for financial support.

REFERENCES

- (1) Kloxin, A. M.; Anseth, K. S. *Nature* **2008**, *454*, 705–706.
- (2) Kloxin, A. M.; Kasko, A. M.; Salinas, C. N.; Anseth, K. S. *Science* **2009**, *324*, 59–63.
- (3) Peppas, N. A.; Huang, Y.; Torres-Lugo, M.; Ward, J. H.; Zhang, J. *Annu. Rev. Biomed. Eng.* **2000**, *2*, 9–29.
- (4) Langer, R.; Tirrell, D. A. *Nature* **2004**, *428*, 487–492.

- (5) Zhang, Z.; Chao, T.; Liu, L. Y.; Cheng, G.; Ratner, B. D.; Jiang, S. Y. *J. Biomater. Sci., Polym. Ed.* **2009**, *20*, 1845–1859.
- (6) Xue, W.; Huglin, M. B.; Liao, B.; Jones, T. G. *J. Eur. Polym. J.* **2007**, *43*, 915–927.
- (7) Susanto, H.; Ulbricht, M. *Langmuir* **2007**, *23*, 7818–7830.
- (8) Carr, L. R.; Xue, H.; Jiang, S. Y. *Biomaterials* **2011**, *32*, 961–968.
- (9) Carr, L. R.; Zhou, Y.; Krause, J. E.; Xue, H.; Jiang, S. *Biomaterials* **2011**, *32*, 6893–6899.
- (10) Hoffman, A. S. *Adv. Drug. Delivery Rev.* **2002**, *54*, 3–12.
- (11) Georges, P. C.; Janmey, P. A. *J. Appl. Physiol.* **2005**, *98*, 1547–1553.
- (12) Engler, A. J.; Griffin, M. A.; Sen, S.; Bonnetnann, C. G.; Sweeney, H. L.; Discher, D. E. *J. Cell Biol.* **2004**, *166*, 877–887.
- (13) Flanagan, L. A.; Ju, Y. E.; Marg, B.; Osterfield, M.; Janmey, P. A. *NeuroReport* **2002**, *13*, 2411–2415.
- (14) Bryant, S. J.; Bender, R. J.; Durand, K. L.; Anseth, K. S. *Biotechnol. Bioeng.* **2004**, *86*, 747–755.
- (15) Moran, J. M.; Pazzano, D.; Bonassar, L. J. *Tissue Eng.* **2003**, *9*, 63–70.
- (16) Teng, Y. D.; Lavik, E. B.; Qu, X. L.; Park, K. I.; Ourednik, J.; Zurakowski, D.; Langer, R.; Snyder, E. Y. *Proc. Natl. Acad. Sci.* **2002**, *99*, 3024–3029.
- (17) Woerly, S.; Doan, V. D.; Sosa, N.; de Vellis, J.; Espinosa-Jeffrey, A. *J. Neurosci. Res.* **2004**, *75*, 262–272.
- (18) Huang, T.; Xu, H. G.; Jiao, K. X.; Zhu, L. P.; Brown, H. R.; Wang, H. L. *Adv. Mater.* **2007**, *19*, 1622–1626.
- (19) Carr, L.; Cheng, G.; Xue, H.; Jiang, S. Y. *Langmuir* **2010**, *26*, 14793–14798.
- (20) Gong, J. P.; Katsuyama, Y.; Kurokawa, T.; Osada, Y. *Adv. Mater.* **2003**, *15*, 1155–1158.
- (21) Tanaka, Y.; Gong, J. P.; Osada, Y. *Prog. Polym. Sci.* **2005**, *30*, 1–9.
- (22) Chiessi, E.; Cavalieri, F.; Paradossi, G. *J. Phys. Chem. B* **2007**, *111*, 2820–2827.
- (23) Jang, S. S.; Goddard, W. A.; Kalani, M. Y. S. *J. Phys. Chem. B* **2007**, *111*, 1729–1737.
- (24) Jang, S. S.; Goddard, W. A.; Kalani, M. Y. S.; Myung, D.; Frank, C. W. *J. Phys. Chem. B* **2007**, *111*, 14440–14440.
- (25) Wang, Q.; Mynar, J. L.; Yoshida, M.; Lee, E.; Lee, M.; Okuro, K.; Kinbara, K.; Aida, T. *Nature* **2010**, *463*, 339–343.
- (26) He, Y.; Shao, Q.; Tsao, H. K.; Chen, S. F.; Goddard, W. A.; Jiang, S. Y. *J. Phys. Chem. B* **2011**, *115*, 11575–11580.
- (27) Plimpton, S. J. *Comput. Phys.* **1995**, *117*, 1–19.
- (28) Plimpton, S. J.; Pollock, R.; Stevens, M. In *Proceedings of the Eighth SIAM Conference on Parallel Processing for Scientific Computing*, Minneapolis, MN, 1997.
- (29) Swope, W. C.; Andersen, H. C.; Berens, P. H.; Wilson, K. R. *J. Chem. Phys.* **1982**, *76*, 637–649.
- (30) Hockney, R. W.; Eastwood, J. W. *Computer Simulation Using Particles*; McGraw-Hill International Book Corporation: New York, 1981.
- (31) Dauberosguthorpe, P.; Roberts, V. A.; Osguthorpe, D. J.; Wolff, J.; Genest, M.; Hagler, A. T. *Proteins* **1988**, *4*, 31–47.
- (32) *Jaguar 4.1*; Schrödinger, Inc.: Portland, OR, 2000.
- (33) Berendsen, H. J. C.; Grigera, J. R.; Straatsma, T. P. *J. Phys. Chem.* **1987**, *91*, 6269–6271.
- (34) Pascal, T. A.; He, Y.; Jiang, S. Y.; Goddard, W. A. *J. Phys. Chem. Lett.* **2011**, *2*, 1757–1760.